ANTIOXIDANTS & REDOX SIGNALING
Volume 8, Numbers 3 & 4, 2006

Forum Review

Measuring Intracellular Redox Conditions Using GFP-Based Sensors

OLOF BJÖRNBERG,[1,2] HENRIK ØSTERGAARD,[3] and JAKOB R. WINTHER[1,4]

ABSTRACT

Recent years have seen the development of methods for analyzing the redox conditions in specific compartments in living cells. These methods are based on genetically encoded sensors comprising variants of Green Fluorescent Protein in which vicinal cysteine residues have been introduced at solvent-exposed positions. Several mutant forms have been identified in which formation of a disulfide bond between these cysteine residues results in changes of their fluorescence properties. The redox sensors have been characterized biochemically and found to behave differently, both spectroscopically and in terms of redox properties. As genetically encoded sensors they can be expressed in living cells and used for analysis of intracellular redox conditions; however, which parameters are measured depends on how the sensors interact with various cellular redox components. Results of both biochemical and cell biological analyses will be discussed. *Antioxid. Redox Signal.* 8, 354–361.

INTRODUCTION

THIOL-DISULFIDE REDOX CHEMISTRY is unique in living systems for its quasi-labile nature. There are two properties of this chemistry which set it aside: (a) the susceptibility of thiols to oxidation by molecular oxygen in our external environment and by reactive oxygen species inside living cells, and (b) the relative promiscuity of thiol-disulfide interchange reactions. In an oxidizing atmosphere the former can be regarded as a general nuisance to biochemical analysis. It is, however, also a key virtue of the major cellular thiol, glutathione, which thus acts as an antioxidant in living cells. The promiscuity aspect of thiol-disulfide reactions has often led to the notion that thiol-disulfide pools are at mutual equilibrium, although this is most likely far from true. Not only are there several thiol redox systems at play within a given compartment that are not at equilibrium with one another; individual compartments are also highly diverse in their redox conditions. This poses particular problems when one tries to assert the cellular redox status for a redox pair, for example, the glutathione/glutathione disulfide pair (GSH and GSSG, respectively). The ratio between the oxidized and reduced forms in a total cell extract disguises large differences between different compartments, a fact that exposes a need for nondisruptive tools for the analysis of redox conditions.

The present review will discuss recent advances in the development of genetically encoded sensors for intracellular redox conditions. We will focus on GFP-based sensors developed independently in two laboratories and compare their characteristics and results from their application *in vivo*. We will also focus on the many potential pitfalls that should be taken into consideration whe\n venturing into intracellular redox sensing.

[1]Carlsberg Laboratory, Copenhagen Valby, Denmark.
[2]Present address: Department of Cell and Organism Biology, Lund University, Lund, Sweden.
[3]Novo Nordisk A/S, Måløv, Denmark.
[4]Present address: Department of Biochemistry, Institute of Molecular Biology and Physiology, Copenhagen, Denmark.

CONSTRUCTION OF GREEN FLUORESCENT PROTEIN-BASED REDOX SENSORS

Biochemical properties of Green Fluorescent Protein (GFP)

GFP was first identified in 1962 by Shimomura and coworkers as a green fluorescing proteinaceous component in extracts of the hydrozoan jellyfish *Aequorea victoria* (21). GFP derives its name from the greenish fluorescence emitted upon illumination of the protein with long-wavelength ultraviolet or blue light. *Aequorea* GFP is a soluble single-chain protein of 27 kDa (17). In the following the term *GFP* will refer to the generic GFP structure encompassing all variants derived from the original wild-type *Aequorea* GFP (wtGFP).

The structure consists of a characteristic 11-stranded β-barrel enclosing a central irregular α-helix, which runs through the barrel and spans its entire length. The fluorescence properties of wtGFP are due to a centrally buried 4-(*p*-hydroxybenzylidene) imidazolidin-5-one chromophore formed posttranslationally by a self-catalyzed intramolecular cyclization of the polypeptide backbone of three residues, Ser65-Tyr66-Gly67, in the central α-helix (Fig. 1A). Heterologous expression of the functional protein in a wide variety of prokaryotic and eukaryotic cells as well as *de novo* chemical synthesis have demonstrated that chromophore formation proceeds independently of any exogenous factors except for molecular oxygen.

The β-barrel itself is almost cylindrical with a height of ~42 Å and an ellipsoidal cross section measuring ~25 x 35 Å^2. The chain-fold topology is shown in Figure 1B. The N-terminal half comprises two β-meanders (strands 1–3 and 4–6) connected by the central α-helix. The polypeptide chain then crosses to the opposite side at the top of the barrel and terminates in a five-stranded Greek key motif (strands 7–11). Except for strand 1 and 6, the β-strands are arranged in an antiparallel fashion. The regular interstrand hydrogen bonding pattern, however, is disrupted between strand 7 and 8, where a bulge is created around the side chain of His148 (strand 7). This site is highly important in determining the spectral properties of GFP due to its close proximity to the phenolic hydroxyl group of the chromophore. The chromophore is completely encapsulated in the interior of the barrel, which has been termed a "β-*can*". Upon denaturation of the mature protein, fluorescence is almost completely lost, showing that the protein matrix protects the fluorophore from quenching.

Spectral properties of wtGFP and the variants of GFP used for redox sensors

wtGFP shows two excitation peaks at about 400 (the A-peak) and 475 nm (the B-peak) with a single emission peak at 510 nm. Elimination of the A-peak can be achieved by replacing Ser65 with other small amino acid residues such as Gly, Thr, Cys, or Ala (1, 6). This has the additional effect of slightly red-shifting the excitation and emission peaks. Fluorescence emission from the S65T and other S65 mutants is highly pH-sensitive, displaying a steep decrease in fluorescence as the pH drops below neutrality (4, 8). Absorbance and fluorescence pH titrations of GFP S65T yielded an apparent chromophore pK_a-value of 6.0 (4).

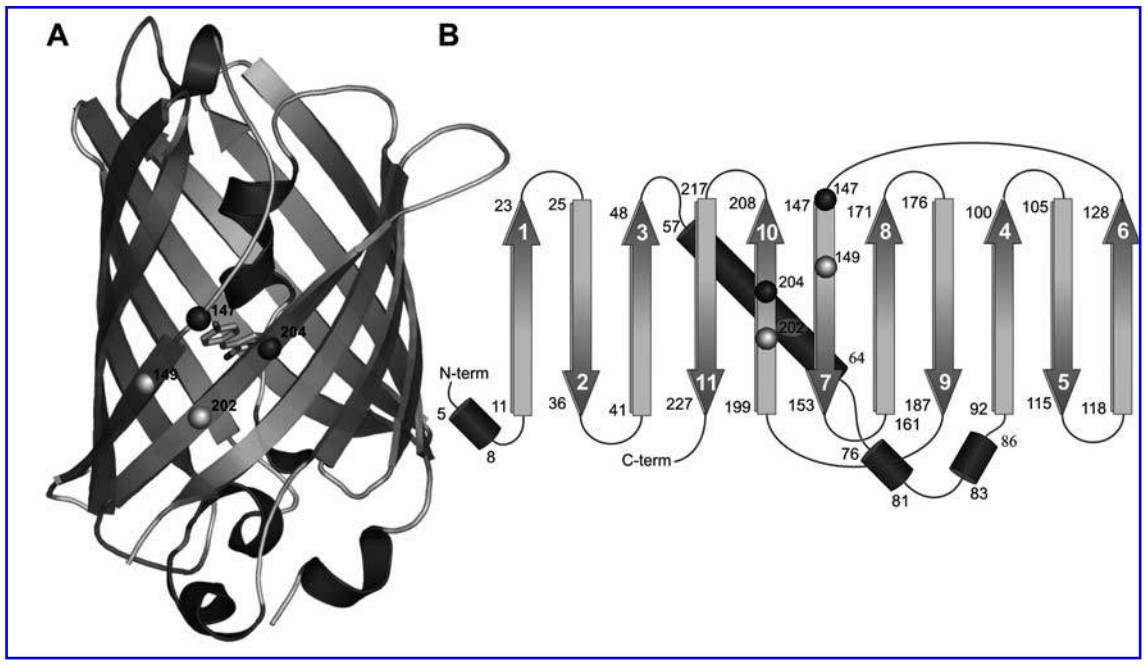

FIG. 1. Position of cysteine residues in the structural layout of GFP. (**A**) Three-dimensional structure of GFP (26) showing the position of cysteine replacements in rxYFP (*white spheres*) and roGFP1 (*dark gray spheres*). The fluorophore, protected from the solvent by the β-barrel structure, is shown in a stick representation. (**B**) In the same gray-scale-code the positions of cysteine substitutions are shown in the topology of the GFP fold.

Additional substitution of Thr203 with Tyr generates Yellow Fluorescent Protein (YFP), the most red-shifted of all known GFP variants, with excitation and emission wavelengths of 512 and 527 nm, respectively (13). The X-ray structure of YFP showed the Tyr203 side chain to stack on top of the phenol group of the chromophore (derived from Tyr66) (25). The close distance between the stacked aromatic side chains (< 3.5 Å) suggests the presence of stabilizing π-π interactions which may explain the significant red-shift of fluorescence (18). Owing to the S65 mutation, the yellow fluorescent proteins are also pH-sensitive. In addition to protons, YFPs are uniquely sensitive to halide ions and other small anions (7).

Due to their unique properties, GFP and its derivatives have gained tremendous interest as noninvasive molecular markers in cell biology. Applications are broadly centered around the use of GFPs as reporters of gene expression (20, 10), protein tracking and interaction (11, 16, 22), and as indicators of biomolecules and cellular activities. Through direct manipulation of GFP as well as fusion to other proteins with desired properties, novel fluorescent proteins have been designed to sense pH, calcium, chloride (halides), metal ions, nitric oxide, protease action, kinase activity, and thiol/disulfide redox potentials amongst others.

Grafting disulfide bonds onto the GFP scaffold

As GFP-sensors can be expressed and assayed in living cells, it was obvious to consider the use of a GFP-based scaffold as a redox sensor. This goal was followed by two groups, independently converging on the same part of GFP for introduction of disulfide bonds (5, 14).

As described above, several residues from strands 7 and 10 in the β-*can* structure extend into the core of the protein and play a key role in defining the spectral properties of GFP and its derivatives. It was therefore attractive to chose these and adjacent strands for introduction of vicinal cysteine residues that were in principle able to form a disulfide bond. It was anticipated that the strain potentially imposed by formation of a disulfide bond would distort the structure in the vicinity of the chromophore in such a way that it would affect the fluorescence.

One group chose to use YFP as template, based on the assumption that the dislocation of Tyr203, unique to the Yellow variant, would affect fluorescence to a significant degree (14). Pairs of cysteine residues were introduced at positions N149-S202, S147-Q204, S202-T225, and Q204-F223. Common to all these pairs is that they protrude from the protein surface into the solvent, allowing them to interact with redox buffers in the environment. For YFP, only the form carrying the N149C-S202C mutations (termed rxYFP, Fig. 1) gave a strong difference in fluorescence signal upon oxidation and reduction. The other cysteine pairs had only modest redox-dependent effects on the fluorescence. Among the four YFP variants constructed, only the Q204C-F223C mutant form showed a significant degree of intermolecular disulfide bond formation.

The other research group chose wtGFP as their starting point for a redox sensor (5). Because GFP has two excitation peaks it was anticipated that this would allow for generation of ratiometric sensors in which the intensity of the A and B peaks would change relatively to each other depending on the degree of disulfide bond formation. They inserted cysteine residues at a subset of the positions used in YFP, S147-Q204 and N149-S202, generating roGFP1 and roGFP3, respectively (Fig. 1). The S65T mutation was introduced into roGFP1 and roGFP3, generating roGFP2 and roGFP4, respectively. As discussed below, the two latter forms have spectral properties different from those of the former two forms.

Interestingly, the structures of rxYFP and roGFP2, containing the 149–202 and 147–204 disulfide bonds, respectively, have both been determined by x-ray crystallography. Not surprisingly, the two structures are superimposable over most of the sequences. However, close to the disulfide bonds there are larger differences, in particular with regard to strand 7, which packs closer towards the core of the protein in the roGFP2 structure than in the rxYFP structure. The distances between strands 7 and 10 at the site of the disulfide are almost identical, as the disulfide bridge in both cases adopts a *right-handed staple* conformation (Fig. 2).

Importantly, the oxidized and reduced forms of rxYFP (and most likely also of roGFP's) can be separated by nonreducing SDS-PAGE. The oxidized state runs faster, most likely due to the hairpin structure formed by linking of widely separated segments of the protein structure. This allows for fluorescence-independent confirmation of the redox state of the sensor under various conditions, but more importantly pulse-labeling experiments allow for determination of the kinetics for attaining steady-state redox levels of the sensor within the cell (14).

Fluorescence properties

The spectral properties of the reduced form of rxYFP are identical to those of YFP while the intensity of the fluores-

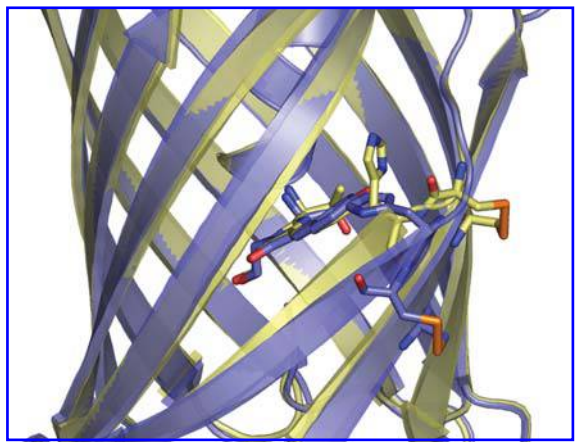

FIG. 2. Structural comparison of rxYFP and roGFP1 in the oxidized state. rxYFP (14) is shown in *blue*, while roGFP2 (5) is in *yellow*. The differences are most significant in strand 10, which is pulled away from the fluorophore. This results in major rearrangements of residues interacting with the fluorophore, most notably His148. Interestingly, the *right-hand staple* conformation of the disulfide bond is almost identical in the two structures. The 149–202 disulfide bond of rxYFP was shown to interact efficiently with the glutaredoxin system (15).

cence of the oxidized form is decreased by approximately the same factor throughout the spectrum. Oxidation of the sensor decreased the peak fluorescence emission at 523 nm by a factor of 2.2. The roGFPs, on the other hand, all show ratiometric behavior. They show the typical A- and B-peaks and a redox-independent isosbestic point at 425 nm. The ratio of the changes at the two peaks, referred to as the dynamic range, is 6.1 and 4.3 for roGFP1 and roGFP3, respectively (5). Relative to roGFP1 and -3, GFP2 and -4 show approximately the inverse relationship of the intensity of the excitation peaks. Also these forms show redox-dependent fluorescence, with ratios of 5.8 and 2.6, respectively (5). Both rxYFP and roGFP2 and -4 are pH-sensitive, exhibiting reduced fluorescence at low pH. The ratiometric behavior of roGFPs is in principle an advantage because it makes the redox determination independent of sensor concentration.

Redox properties

A fundamental property of a disulfide bond is its thermodynamic stability. For any sensor it is of course important that the macroscopic properties that constitute the sensor readout change within a range that is relevant for the conditions to be investigated. This is usually determined from equilibrium constants (K_{ox}) with other thiol-disulfide pairs of known stability. The stability of a disulfide bond is normally expressed as a standard redox potential using the Nernst equation:

$$E'_0(\text{Sensor}) = E'_0(N_{SH/SS}) - (RT/nF)\ln K_{ox} \quad \text{Eq. 1}$$

where $E'_0(N_{SH/SS})$ is the standard redox potential for oxidation of the compound NSH_2 to NSS, R is the gas constant, T is the absolute temperature, n is the number of electrons transferred and F is the Faraday constant. K_{ox} is the equilibrium constant for the reaction:

$$\text{Sensor}_{red} + N_{SS} \Leftrightarrow \text{Sensor}_{ox} + N_{SH} \quad \text{Eq. 2}$$

In the case of the 149–202 disulfide bond, the redox potential was found to be –265 mV of rxYFP (14), –299 mV for roGFP3, and –286 mV for roGFP4 (5). Although the disulfide bond is the same in all three cases, there appears to be some differences that are dependent on the small differences in the protein sequences. In the case of rxYFP, the glutathione (GSH/GSSG) pair ($E'_0 = -240$ mV) was used for determination of the redox potential, while oxidized and reduced DTT was used in the latter cases. Part of the difference can be accounted for by the use of an E'_0 of −323 mV for DTT. A more recent and detailed analysis of the DTT/GSSG redox equilibrium has yielded a less reducing redox potential of −308 mV for DTT (19). Values compensated accordingly are given in Table 1 and are still more reducing than those obtained for rxYFP. It is conceivable that rxYFP is slightly more oxidizing because of the bulkiness of the Tyr203 relative to the Thr found in this position in the roGFPs. This would force strand 7 slightly away from the core of the protein, decreasing the stability of the disulfide bond.

The redox potentials of roGFP1 and -2 have been determined using DTT as well as lipoic acid (6,8-dithiooctanoic acid) and bis(2-mercaptoethyl)sulfone. In general the values obtained with the latter reagents were somewhat more reducing. However, consensus values of −291 and −280 mV are suggested in a later paper (3). These values are more reducing than those found for the 149–202 disulfide bond in rxYFP.

MEASURING REDOX CONDITIONS IN LIVING CELLS

Considerations on intracellular redox homeostasis and redox sensing

Obviously, the sensors exit the ribosome in the reduced state and as such must react with intracellular constituents to

TABLE 1. MUTATIONS AND REDOX PROPERTIES OF SENSORS

Redox sensor	*Disulfide bond*	*Mutations relative to wtGFP*	*E'0 (mV)*	*Kox[c] (GSH²/GSSG)*
rxYFP	149–202	S65A C48V Q80R N149C M153V S202C T203Y D234H	−265	6.8
roGFP1	147–204	C48S Q80R S147C Q204C	−291[a]	50
roGFP2	147–204	C48S Q80R S65T S147C Q204C	−280[a]	21
roGFP3	149–202	C48S Q80R N149C S202C	−299 (−284[b])	29
roGFP4	149–202	C48S Q80R S65T N149C S202C	−286 (−271[b])	10.7 10.7

[a] Consensus value suggested by Dooley *et al.* (3).
[b] Original E'_0 revised in accordance with an E'_0 (DTT) of –308 mV, as derived from Rothwarf and Scheraga (19).
[c] Calculated based on a E'_0 of −240 mV for the GSH/GSSG pair.

attain a steady-state level of oxidation. While the use of rxYFP and roGFPs in living cells may yield data that can be used to describe redox conditions *ad hoc*, some issues regarding their interaction with the cellular environment can be addressed already from a theoretical point of view. The cellular redox milieu is made up of numerous redox pairs each defining a redox potential. For instance, it is known that the $NADPH/NADP^+$ and $NADH/NAD^+$ ratios can be very different (e.g., 5.3 and 0.15 in anaerobically grown yeast) although these redox pairs have almost identical standard redox potentials (12). For redox pools that are not at mutual equilibrium, the redox status of a sensor will be determined by kinetic factors (i.e., the rates by which it equilibrates with the individual pools). If it equilibrates with a strong preference with one pool over another, it will in effect be a sensor for the former redox pool.

In the eukaryotic cytosol, glutaredoxins and thioredoxins are the enzymes that are primarily responsible for maintaining protein thiols in the reduced state (Fig. 3). Glutaredoxins derive their reducing equivalents from reduced glutathione, which is found in cells at m*M* concentrations. Oxidized glutathione is generated by various oxidative processes and is continuously reduced by the enzyme glutathione reductase at the expense of NADPH.

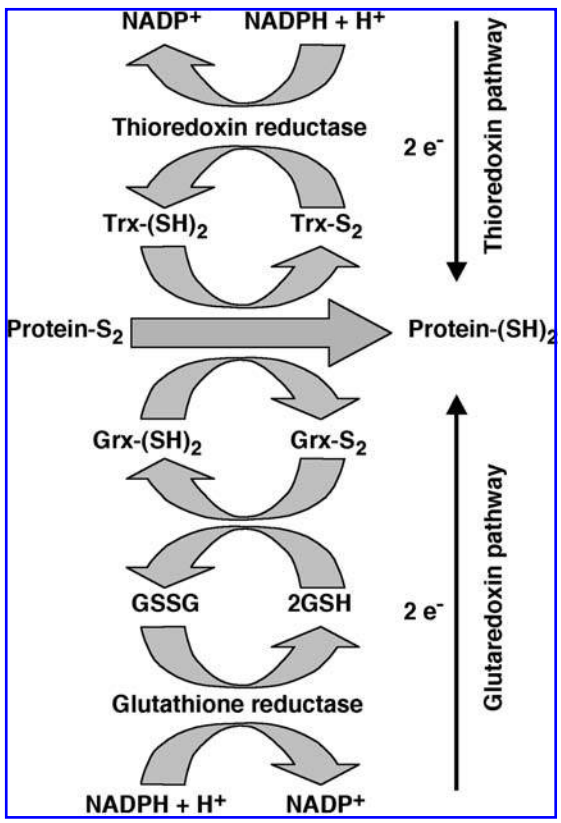

FIG. 3. Thioredoxin/glutaredoxin pathways of reduction of protein disulfides. While the thioredoxin system (*above the horizontal arrow*) relies on a proteinaceous catalyst in every step, the glutaredoxin system (*below the horizontal arrow*) acts via the GSH/GSSG redox buffer. $Trx(SH)_2$ and $TrxS_2$ indicate the reduced and oxidized forms, respectively, of thioredoxin. Likewise, $Grx(SH)_2$ and $GrxS_2$ indicate the reduced and oxidized forms, respectively, of glutaredoxin. The *arrows* show the direction of electron flow.

Functioning in parallel with this system is the thioredoxin system. Importantly, the thioredoxin system does not employ a low molecular weight thiol redox buffer. Its reduction is directly linked to the oxidation of NADPH through the enzyme thioredoxin reductase. This enzymatic link of thioredoxin, with an $E'_0 = -270$ mV, to NADPH, with $E'_0 = -315$ mV, generates an extremely powerful reducing system (9). Assay of the intracellular redox state of thioredoxin in the yeast cytosol has shown this enzyme to be almost exclusively in the reduced state (24). This means that thioredoxin acts as a sink of oxidizing equivalents for almost any disulfide bond that it interacts efficiently with. Glutaredoxin, on the other hand, in effect only acts to equilibrate interacting thiols and disulfides with the glutathione redox buffer.

To illustrate the crucial importance of understanding which pathways a redox sensor interacts with, we would like to point to recent data on the mechanism of the Yap1p transcription factor from yeast. Yap1p is a basic leucine zipper transcription factor that in response to H_2O_2 activates genes that code for antioxidants including enzymes in the thioredoxin and glutaredoxin family. In Yap1p, a disulfide bond between cysteine residues 303 and 598 is formed upon exposure of cells to H_2O_2 (23). This leads to unmasking of a nuclear localization signal and transfer of Yap1p to the nucleus, where is activates target genes. Interestingly, the 303–598 disulfide bond is formed rapidly and highly specifically by the enzyme Orp1p, which itself acts as a H_2O_2 receptor (2). Over a period of 30–45 minutes, the 303–598 disulfide bond will be reduced by thioredoxin. This indicates that the pathway is under kinetic control and that an increase of the level of active Yap1p only occurs if the rate of oxidation by Orp1p is faster than the rate of reduction by thioredoxin.

Because of the direct enzymatic link to NADPH oxidation, we would expect a redox sensor to be much more reduced if it was a good substrate for thioredoxin than if the glutathione pool determined its redox state.

The redox state of rxYFP in the yeast cytosol

About 10% of rxYFP molecules were found by fluorescence measurements to be oxidized in the yeast cytosol under steady-state conditions. The degree of fluorescence is determined by comparing the initial fluorescence of a cell suspension with that of a fully oxidized sample (after treatment of cells with 4,4′-dipyridyl disulfide (4-DPS)) and a fully reduced sample (after treatment of the same cells with excess DTT). Using a combination of genetics and pulse-labeling techniques (separating oxidized forms from reduced forms on non-reducing SDS-PAGE, as described above) it was seen that rxYFP reaches its steady-state oxidation level more slowly in mutants lacking glutaredoxin. Furthermore, while glutaredoxin 1 from yeast readily equilibrates rxYFP with a glutathione redox buffer *in vitro*, no thiol-disulfide exchange between rxYFP and purified thioredoxins (Trx1p and Trx2p from yeast) was detected (15). Thus, rxYFP equilibrates with a glutathione redox buffer through the action of glutaredoxin (Fig. 4). Contrary to the generally assumed role of the en-

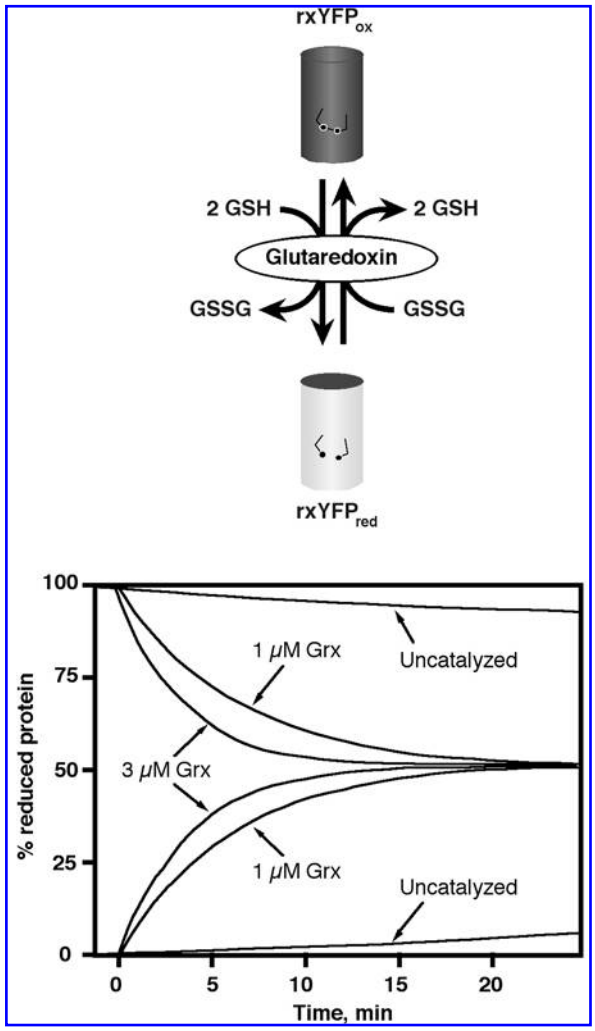

FIG. 4. Yeast glutaredoxin 1 catalyzes equilibration of rxYFP with a glutathione redox buffer. The reversible reaction of GSH and GSSG with oxidized and reduced rxYFP, respectively, is catalyzed by the glutaredoxin encoded by the yeast GRX1 gene. That this is indeed the case is shown in the *bottom panel* where either oxidized or reduced rxYFP is placed in a redox buffer with the same redox potential as rxYFP. At equilibrium this will result in rxYFP being 50% oxidized. The uncatalyzed reactions are rather slow, requiring several hours to reach equilibrium, while addition of yeast glutaredoxin 1 results in a strong rate enhancement (adapted from (15)).

zyme, glutaredoxin in this case catalyzes the *formation* of a disulfide bond in the newly synthesized rxYFP (Fig. 3).

It should also be noted that while fluorescence measurements showed the fraction of oxidized rxYFP to be about 10%, pulse-labeling experiments resulted in 14–15% oxidized rxYFP. This underestimation of the amount of GSSG by the steady-state fluorescence measurement can be explained by the fact that the redox sensor is initially synthesized in the reduced state. Therefore, in systems with high growth rates the rate of oxidation may be comparable to the production rate of sensor and this must be taken into account in steady-state measurements. With the latter percentage the cytosolic redox potential of the glutathione pool could be determined as –289 mV. Because the redox potential is determined by the $[GSH]^2/[GSSG]$ ratio, neither the absolute concentrations nor the GSH/GSSG ratios can be directly derived from the degree of oxidation. However, using chemical determination of GSH and GSSG in whole cell extracts and more complicated kinetic data derived from mutants lacking glutaredoxins, the cytosolic levels of glutathione were estimated to be ≈13 m*M* GSH and ≈4 μ*M* GSSG in the wild-type yeast cytosol. However, the single most important property of the readout from rxYFP is that it, at least in yeast cells, refers to a specific redox pair, namely that of GSH and GSSG.

The redox state of roGFPs in HeLa cells

To gauge the effects of different oxidants on the roGFP1 and roGFP2 sensors Dooley *et al.* performed dose-response experiments that assayed the effect of different oxidants *in vitro* (3). They found that roGFP2 ($E_0' = -280$ mV) was generally oxidized faster at lower concentrations of oxidants than roGFP1 (−291 mV), despite being less reducing. This observation shows how important kinetic effects may be, as one would expect the more reducing protein to be oxidized more rapidly. The redox-state changes of roGFPs *in vivo* are also clearly influenced by interacting enzymes as seen from experiments set up to simulate oxidative stress conditions. For roGFP2, the responses (i.e., the rates of oxidation) upon exposure to H_2O_2 and superoxide were much faster *in vivo* than *in vitro* although the compound had to cross membranes (3). The different placement of the disulfide bond in roGFP1 and -2 relative to rxYFP might enable interaction with thioredoxin. Indeed, a link to the thioredoxin/NADPH system is indicated by "washout experiments" of HeLa cells. Cytoplasmic roGFP2 was oxidized by 100 μ*M* DPS and the subsequent reduction of the sensor was followed after washout of the reagent. Pretreatment of the cells with inhibitors of thioredoxin reductase and dihydrolipoamide dehydrogenase, cisplatin and 5-methoxyindole-2-carboxylic acid, respectively, blocked re-reduction of the sensor. The former inhibitor would inhibit reduction of thioredoxin while the latter would affect the reduction of $NADP^+$. However, these apparent links to the thioredoxin system might be indirect since NADPH is required for the turnover of GSSG. Other experiments might suggest that roGFPs interact with glutaredoxins. Pretreatment of HeLa cells with buthione sulfoximine, an inhibitor of GSH synthesis, and aminotriazole, a catalase inhibitor, increased the fluorescence responses to H_2O_2. The cellular defense against H_2O_2 and other peroxides comprises a variety of enzymes. Catalase acts independently, whereas other peroxidases are supported with reducing equivalents from either the thioredoxin or glutaredoxin system. Thus, it remains unclear whether roGFPs in mammalian cells are primarily targets of thioredoxin or glutaredoxin or whether there even is a competition between the two.

The fraction of oxidized sensor as determined by fluorescence in yeast cells (≈10% implying –294 mV) can be compared to the 16% and 5% of roGFP1 and −2, implying −315 and −325 mV, respectively, in the cytoplasm of HeLa cells (3). Furthermore, Hanson *et al.* investigated the mitochondrial redox state using roGFP1 containing a targeting se-

quence (5). Assuming a mitochondrial pH of 8.0 at 37°C, −360 mV was obtained. If these values reflect the glutathione redox potential, the −315 mV of cytosolic roGFP1, would indicate a GSSG concentration of ~0.2 μ*M*, assuming that the concentration of GSH is the same as in yeast cells.

It may well be that human glutaredoxins equilibrate the glutathione pool with roGFP1 and -2. In this case the redox state of roGFP would reflect a significantly lower redox potential in HeLa cells than in yeast cells. Alternatively, the rate of equilibration with the glutathione buffer may be so slow that the equilibrium end-point is significantly more oxidized than indicated by fluorescence measurements. On the other hand, significant interaction with thioredoxins means that roGFP1 and -2 instead to a large extent would read the redox state of the thioredoxin system.

FUTURE PERSPECTIVES

Obviously, the redox sensors described in this review open up a wealth of new possibilities for detecting differences in redox milieu between compartments as well as the effects on cells of changes in their environment. Due to the potentially slow reaction of the current sensors with glutathione it should, however, be emphasized that a sensor does not necessarily measure the redox status of glutathione. In order to do so, the given system should harbor a catalyst for the redox-equilibration with glutathione in the form of glutaredoxin. It is here interesting to note that not all glutaredoxins catalyze equilibration of rxYFP, for example, glutaredoxin 2 from *E. coli* is essentially inert towards rxYFP (O. Björnberg, H. Østergaard, and J. R. Winther, unpublished observations). The reactivity of a thiol is determined by its pK_a. By insertion of positive charges in the vicinity of the disulfide bond in rxYFP its reactivity can be increased by up to 13-fold towards glutathione (R. Hansen, H. Østergaard and J.R. Winther, manuscript submitted). This may circumvent the need for an endogenous catalyst, but may enhance possible problems of specificity.

If specificity towards thioredoxin (and *not* glutaredoxin) can be shown for roGFP1 and -2 this would give interesting insight into the dynamics of the thioredoxin system, which is not currently available.

All the five redox sensors described here have very reducing standard redox potentials (e. g., the redox potential of rxYFP is such that in a 10 m*M* GSH solution the sensor will go from 10% oxidized to 90% oxidized when the GSSG concentration is varied from 1.5 μ*M* GSSG to 180 μ*M* GSSG). This, so to speak, defines the practical range of the sensor. Whereas this turned out to be useful for determining the redox potential for the cytoplasmic glutathione pool in a eukaryotic cell, these sensors are not suitable for determining redox conditions in more oxidizing compartments of the cell, such as the endoplasmic reticulum or other parts of the secretory pathway. Indeed rxYFP is almost completely oxidized in the yeast endoplasmic reticulum (H. Østergaard, C. Tachibana, and J.R. Winther, unpublished observations). Determination of glutathione redox status in these compartments is highly interesting but would require modification of the sensors towards more oxidizing redox potentials (i.e., less stable disulfide bonds).

ACKNOWLEDGMENTS

The authors thank Morten C. Kielland-Brandt and Christine Tachibana for critical reading of the manuscript.

ABBREVIATIONS

DTT, dithiothreitol; GFP, green fluorescent protein; roGFP, redox sensitive green fluorescent protein; rxYFP, redox sensitive yellow fluorescent protein; YFP, yellow fluorescent protein.

REFERENCES

1. Delagrave S, Hawtin RE, Silva CM, Yang MM, and Youvan DC. Red-shifted excitation mutants of the green fluorescent protein. *Biotechnology (NY)* 13: 151–154, 1995.
2. Delaunay A, Pflieger D, Barrault MB, Vinh J, and Toledano MB. A thiol peroxidase is an H_2O_2 receptor and redox-transducer in gene activation. *Cell* 111: 471–481, 2002.
3. Dooley CT, Dore TM, Hanson GT, Jackson WC, Remington SJ, and Tsien RY. Imaging dynamic redox changes in mammalian cells with green fluorescent protein indicators. *J Biol Chem* 279: 22284–22293, 2004.
4. Elsliger MA, Wachter RM, Hanson GT, Kallio K, and Remington SJ. Structural and spectral response of green fluorescent protein variants to changes in pH. *Biochemistry* 38: 5296–5301, 1999.
5. Hanson GT, Aggeler R, Oglesbee D, Cannon M, Capaldi RA, Tsien RY, and Remington SJ. Investigating mitochondrial redox potential with redox-sensitive green fluorescent protein indicators. *J Biol Chem* 279: 13044–13053, 2004.
6. Heim R and Tsien RY. Engineering green fluorescent protein for improved brightness, longer wavelengths and fluorescence resonance energy transfer. *Curr Biol* 6: 178–182, 1996.
7. Jayaraman S, Haggie P, Wachter RM, Remington SJ, and Verkman AS. Mechanism and cellular applications of a green fluorescent protein-based halide sensor. *J Biol Chem* 275: 6047–6050, 2000.
8. Kneen M, Farinas J, Li Y, and Verkman AS. Green fluorescent protein as a noninvasive intracellular pH indicator. *Biophys J* 74: 1591–1599, 1998.
9. Krause G, Lundstrom J, Barea JL, de la Cuesta P, and Holmgren A. Mimicking the active site of protein disulfide-isomerase by substitution of proline 34 in *Escherichia coli* thioredoxin. *J Biol Chem* 266: 9494–9500, 1991.
10. Leveau JH and Lindow SE. Predictive and interpretive simulation of green fluorescent protein expression in reporter bacteria. *J Bacteriol* 183: 6752–6762, 2001.
11. Margolin W. Green fluorescent protein as a reporter for macromolecular localization in bacterial cells. *Methods* 20: 62–72, 2000.
12. Nissen TL, Anderlund M, Nielsen J, Villadsen J, and Kielland-Brandt MC. Expression of a cytoplasmic transhydrogenase in *Saccharomyces cerevisiae* results in forma-

tion of 2-oxoglutarate due to depletion of the NADPH pool. *Yeast* 18: 19–32, 2001.
13. Ormo M, Cubitt AB, Kallio K, Gross LA, Tsien RY, and Remington SJ. Crystal structure of the *Aequorea victoria* green fluorescent protein. *Science* 273: 1392–1395, 1996.
14. Østergaard H, Henriksen A, Hansen FG, and Winther JR. Shedding light on disulfide bond formation: engineering a redox switch in green fluorescent protein. *EMBO J* 20: 5853–5862, 2001.
15. Østergaard H, Tachibana C, and Winther JR. Monitoring disulfide bond formation in the eukaryotic cytosol. *J Cell Biol* 166: 337–345, 2004.
16. Phillips GJ. Green fluorescent protein—a bright idea for the study of bacterial protein localization. *FEMS Microbiol Lett* 204: 9–18, 2001.
17. Prasher DC, Eckenrode VK, Ward WW, Prendergast FG, and Cormier MJ. Primary structure of the *Aequorea victoria* green-fluorescent protein. *Gene* 111: 229–233, 1992.
18. Remington SJ. Structural basis for understanding spectral variations in green fluorescent protein. *Methods Enzymol* 305: 196–211, 2000.
19. Rothwarf DM and Scheraga HA. Equilibrium and kinetic constants for the thiol-disulfide interchange reaction between glutathione and dithiothreitol. *Proc Natl Acad Sci USA* 89: 7944–7948, 1992.
20. Scholz O, Thiel A, Hillen W, and Niederweis M. Quantitative analysis of gene expression with an improved green fluorescent protein. *Eur J Biochem* 267: 1565–1570, 2000.
21. Shimomura O, Johnson FH, and Saiga Y. Extraction, purification and properties of aequorin, a bioluminescent protein from the luminous hydromedusan, Aequorea. *J Cell Comp Physiol* 59: 223–239, 1962.
22. Tavare JM, Fletcher LM, and Welsh GI. Using green fluorescent protein to study intracellular signalling. *J Endocrinol* 170: 297–306, 2001.
23. Toledano MB, Delaunay A, Monceau L, and Tacnet F. Microbial H_2O_2 sensors as archetypical redox signaling modules. *Trends Biochem Sci* 29: 351–357, 2004.
24. Trotter EW and Grant CM. Non-reciprocal regulation of the redox state of the glutathione- glutaredoxin and thioredoxin systems. *EMBO Rep* 4: 184–188, 2003.
25. Wachter RM, Elsliger MA, Kallio K, Hanson GT, and Remington SJ. Structural basis of spectral shifts in the yellow-emission variants of green fluorescent protein. *Structure* 6: 1267–1277, 1998.
26. Yang F, Moss LG, and Phillips GN Jr. The molecular structure of green fluorescent protein. *Nat Biotechnol* 14: 1246–1251, 1996.

Address reprint requests to:
Jakob R. Winther
Department of Biochemistry
Institute of Molecular Biology and Physiology
August Krogh Building
Universitetsparken 13
DK-2100 Copenhagen, Denmark.

E-mail: jrwinther@aki.ku.dk

Received after revision February 7, 2005; accepted April 5, 2005.

This article has been cited by:

1. Masahide Oku , Yasuyoshi Sakai . 2012. Assessment of Physiological Redox State with Novel FRET Protein Probes. *Antioxidants & Redox Signaling* **16**:7, 698-704. [Abstract] [Full Text HTML] [Full Text PDF] [Full Text PDF with Links]
2. Marcel Deponte. 2012. GFP tagging sheds light on protein translocation: implications for key methods in cell biology. *Cellular and Molecular Life Sciences* . [CrossRef]
3. Frank Funke, Florian J. Gerich, Michael Müller. 2011. Dynamic, semi-quantitative imaging of intracellular ROS levels and redox status in rat hippocampal neurons. *NeuroImage* **54**:4, 2590-2602. [CrossRef]
4. Chunchen Lin, Vladimir L. Kolossov, Gene Tsvid, Lisa Trump, Jennifer Jo Henry, Jerrod L. Henderson, Laurie A. Rund, Paul J.A. Kenis, Lawrence B. Schook, H. Rex Gaskins, Gregory Timp. 2011. Imaging in real-time with FRET the redox response of tumorigenic cells to glutathione perturbations in a microscale flow. *Integrative Biology* **3**:3, 208. [CrossRef]
5. Kristine Steen Jensen , Rosa E. Hansen , Jakob R. Winther . 2009. Kinetic and Thermodynamic Aspects of Cellular Thiol–Disulfide Redox Regulation. *Antioxidants & Redox Signaling* **11**:5, 1047-1058. [Abstract] [Full Text PDF] [Full Text PDF with Links]
6. Kairit Zovo , Peep Palumaa . 2009. Modulation of Redox Switches of Copper Chaperone Cox17 by Zn(II) Ions Determined by New ESI MS-Based Approach. *Antioxidants & Redox Signaling* **11**:5, 985-995. [Abstract] [Full Text PDF] [Full Text PDF with Links]
7. R. Dumollard, J. Carroll, M.R. Duchen, K. Campbell, K. Swann. 2009. Mitochondrial function and redox state in mammalian embryos. *Seminars in Cell & Developmental Biology* **20**:3, 346-353. [CrossRef]
8. Sabina Bednarska, Pierre Leroy, Marek Zagulski, Grzegorz Bartosz. 2008. Efficacy of antioxidants in the yeast Saccharomyces cerevisiae correlates with their effects on protein thiols. *Biochimie* **90**:10, 1476-1485. [CrossRef]
9. A MEYER. 2008. The integration of glutathione homeostasis and redox signaling. *Journal of Plant Physiology* **165**:13, 1390-1403. [CrossRef]
10. M. SCHWARZLÄNDER, M.D. FRICKER, C. MÜLLER, L. MARTY, T. BRACH, J. NOVAK, L.J. SWEETLOVE, R. HELL, A.J. MEYER. 2008. Confocal imaging of glutathione redox potential in living plant cells. *Journal of Microscopy* **231**:2, 299-316. [CrossRef]
11. Andreas J. Meyer, Thorsten Brach, Laurent Marty, Susanne Kreye, Nicolas Rouhier, Jean-Pierre Jacquot, Rüdiger Hell. 2007. Redox-sensitive GFP in Arabidopsis thaliana is a quantitative biosensor for the redox potential of the cellular glutathione redox buffer. *The Plant Journal* **52**:5, 973-986. [CrossRef]
12. Christian Schwarzer, Beate Illek, Jung H. Suh, S. James Remington, Horst Fischer, Terry E. Machen. 2007. Organelle redox of CF and CFTR-corrected airway epithelia. *Free Radical Biology and Medicine* **43**:2, 300-316. [CrossRef]
13. Dr. Marat V. Avshalumov , Li Bao , Jyoti C. Patel , Margaret E. Rice . 2007. H2O2 Signaling in the Nigrostriatal Dopamine Pathway Via ATP-Sensitive Potassium Channels: Issues and Answers. *Antioxidants & Redox Signaling* **9**:2, 219-231. [Abstract] [Full Text PDF] [Full Text PDF with Links]
14. Marat V. Avshalumov, Li Bao, Jyoti C. Patel, Margaret E. Rice. 2006. H 2 O 2 Signaling in the Nigrostriatal Dopamine Pathway Via ATP-Sensitive Potassium Channels: Issues and Answers. *Antioxidants & Redox Signaling*, ahead of print061121054212001. [CrossRef]
15. Dr. , Adam M. Benham , Roberto Sitia . 2006. The Diversity of Oxidative Protein Folding. *Antioxidants & Redox Signaling* **8**:3-4, 271-273. [Citation] [Full Text PDF] [Full Text PDF with Links]